NMR Structural Study on the As−P−S Glassy System

S. H. Santagneli, I. Skripatchev, S. J. L. Ribeiro, and Y. Messaddeq*

Institute of Chemistry − UNESP, P.O. Box 355, Araraquara, SP 14801-970, Brazil

J. Schneider

Instituto de Física de São Carlos, Universidade de São Paulo, Av. Trabalhador Saocarlense 400, São Carlos, SP 13566-590, Brazil

Received February 21, 2007. Revised Manuscript Received July 24, 2007

Glasses having the composition $As_2S_{3(1-x)}-P_2S_{5(x)}$ with x ranging from 0 to 0.7 have been investigated to determine the compositional effect on properties and local structure. Glass transition temperature (T_g) decreases and molar volume (V_m) increases with an increase in P content. Using ^{31}P NMR, we measured the strength of the $^{31}P-^{31}P$ magnetic dipolar interaction in the glass samples and the $AsPS_4$ crystallized phase. Based on these data, we observed the formation of the $As_2P_2S_8$ network, which reflects an increase in the average coordination number and a decrease in the degree of rigidity.

I. Introduction

Chalcogenide glasses are well reported in literature and have many applications in the infrared region as optical fibers or optical lasers.[1,2] They also present several interesting properties when submitted to irradiation energy above or under the energy band gap.[3−5] In spite of their technological applications, their structural organization is still not well understood in some glass-forming systems, which is the case for ternary As−P−S.[2] The glass-forming region of this system has already been reported by several authors,[6−8] and they indicate that it has an upper limit of up to 70% of the P_2S_5.[6] It is also known that in the As−P−S system two crystalline phases can be formed as $As_2P_2S_7$, which is constituted of two $S{=}PS_{3/2}$ tetrahedrons interconnected by P−S−P bonding. And the other phase is $AsPS_4$, which consists of a polymeric unit having two $S{=}PS_{3/2}$ groups connected by P−S−P bonding and two $AsS_{3/2}$ trigonal units.[9] Additionally the combination of As and S form two crystalline phases: As_2S_2 and As_2S_3.[10] Along with this, the P−S binary may form several molecular and crystalline phases, such as α-P_4S_3, β-P_4S_3, γ-P_4S_3, P_4S_7, and P_4S_{10}.[11,12] From these facts, it is clear that the combination of As, S, and P may form several crystalline compounds, consisting of many molecular-like groups. These molecular units may be present as building blocks in the glass network. Therefore, it is difficult to obtain structural information from the glass using only Raman and infrared spectroscopy as previously reported.[6,7] Also, Santagneli et al. have reported several interesting photoinduced effects in the ternary system As−P−S depending on exposure time, power density, and radiation wavelength.[13] However, a structural study is necessary to elucidate the origin of such a phenomenon.

The present paper deals with a systematic study of the ternary system As−P−S using solid-state high-resolution Nuclear Magnetic Resonance (NMR) of ^{31}P and spin−echo (SE) techniques. The combination of these techniques gives relevant information about the phosphorus incorporation into the glass network from the analysis of the ^{31}P anisotropic chemical shift interaction and the strength of the magnetic dipolar homonuclear interaction between ^{31}P nuclei.[14−16]

II. Theory

II.1. Homonuclear ^{31}P Magnetic Dipole Interaction. In solids with many interacting spins, the strength of $^{31}P-^{31}P$ magnetic dipole interaction may be characterized by the second moment (M_2) of the broadened NMR line.[17] The M_2 can be related to the interatomic distances using the Van Vleck method.[18] Considering that all the orientations of the

* Corresponding author phone: +55-16 3301 66 32; fax: +55-16 3301 6692; e-mail: younes@iq.unesp.br.

(1) Nishii, J.; Morimoto, S.; Inagawa, I.; Iizuka, R.; Yamashita, T.; Yamagishi, T. *J. Non-Cryst. Solids* **1992**, *140*, 199.
(2) Devyatykh, G. G.; Churbanov, M. F.; Scripachev, I.; Snopatin, G. E. *J. Non-Cryst. Solids* **1999**, *63*, 256−57.
(3) Tanaka, K. *Philos. Mag. Lett.* **1999**, *79* (1), 25.
(4) Tanaka, K. *J. Non-Cryst. Solids* **2000**, *266/269*, 889.
(5) Bloking, J. T.; Krishnaswami, S.; Jain, H.; Vlcek, M.; Vinci, R. P. *Opt. Mater. (Amsterdam)* **2001**, *17*, 453.
(6) Koudelka, L.; Blinov, L. N.; Gutenev, M. S. *J. Non-Cryst. Solids* **1991**, *130*, 236.
(7) Tverjanovich, A.; Kruger, M.; Soltwich, M.; Quitmann, D. *J. Non-Cryst. Solids* **1991**, *134*, 86.
(8) Blachnik, R.; Hoppe, A. *J. Non-Cryst. Solids* **1979**, *34* (2), 191.
(9) Wibbelmann, C.; Brockner, W. *Z. Naturforsch., A: Phys. Sci.* **1981**, *36a*, 836.
(10) Holomb, R. M.; Mitsa, V. M. *J. Optoelectron. Adv. Mater.* **2004**, *6* (4), 1177.
(11) Vos, A.; Wiebenga, E. H. *Acta Crystallogr.* **1995**, *8* (4), 217.
(12) Leung, Y. C.; Waser, J.; Vanhouten, S.; Vos, A.; Wiegers, G. A.; Wiebenga, E. H. *Acta Crystallogr.* **1957**, *10* (9), 574.
(13) Santagneli, S. H. Ph.D. Thesis, Instituto de Química − Araraquara, Universidade Estadual Paulista, 2006.
(14) Lathrop, D.; Eckert, H. *J. Am. Chem. Soc.* **1989**, *111* (10), 3536.
(15) Lathrop, D.; Eckert, H. *Phys. Rev. B: Condens. Matter Mater. Phys.* **1991**, *43* (9), 7279.
(16) Cherry, B. R.; Zwanziger, J. W.; Aitken, B. G. *J. Phys. Chem. B* **2002**, *106*, 11093.
(17) Abragam, A. *Principles of Nuclear Magnetism;* Clarendon Press: Oxford, 1964.

10.1021/cm070496k CCC: $37.00
Published on Web 10/18/2007

internuclear vector with respect to the Zeeman field are equally probable, the Van Vleck theory predicts that for phosphorus nuclei (I=1/2) subjected to strong chemical shift anisotropy the second moment is given by[14,15,18]

$$M_2 = \frac{4}{15}\left(\frac{\mu_0}{4\pi}\right)^2 I(I+1)\gamma^4\hbar^2\frac{1}{N}\sum_{i\neq j} r_{ij}^{-6} \qquad (1)$$

where γ is the giromagnetic ratio, N is the number of interacting spins, and r_{ij} are the internuclear distances. The measurement of M_2 can be done using the Hahn spin−echo pulse sequence $\pi/2$-τ-π, which refocuses all spin interactions linear in I_z. Assuming multiple coupling between the spins, the decay of the spin−echo intensities $I(2\tau)$ due to the non-refocused homonuclear dipolar interaction can be approximated in many circumstances by a Gaussian function.

$$I(2\tau)/I(0) = \exp\{-M_2(2\tau)^2/2\} \qquad (2)$$

In systems where the distribution of spins is not homogeneous, the dipolar coupling can be very different in distinct groups of spins. In this case, the observed spin−echo intensity may be considered as a sum of several contributions, as given by expression 2, each with a particular second moment $M_2^{(i)}$ corresponding to distinct spin groupings.

II.2. Model Distributions of P Atoms in As−P−S Glasses. The values of the second moment and (M_2) the Van Vleck expression can be used to test the state of aggregation, or distribution, of P atoms within the glass structure. Three simplistic models for P distribution were considered in this study, and the M_2 values for each of them were calculated according to expression 1.

II.2.a. Homogeneous Distribution. In this model, P atoms are assumed to be homogeneously dispersed in the glass, maximizing their internuclear distances. Considering the composition and experimental density of these glasses, P−P distances were calculated assuming that P atoms are located at the vertices of a cubic lattice, whose parameter was calculated for each glass as a function of composition and measured density.

II.2.b. Random Distribution. This simplified model, successfully applied by Eckert and co-workers in several chalcogenide systems[14,15] takes into consideration some chemical and structural constraints. It is assumed that the glass structure is a random network composed of $AsS_{3/2}$, $PS_{3/2}$, and $S{=}PS_{3/2}$ units. Within this model, higher values of M_2 are expected as compared with the homogeneous distribution due to the possibility of shorter P−P distances, as for example in P−S−P contacts. A simplified way to carry out the calculations is to consider that As, S, and P atoms are located at the sites of a zinc-blend structure.[14] This lattice provides an easy framework to locate tetrahedral and trigonal sites. The sites of one of the FCC sublattices of the zinc-blend are randomly occupied by As or P atoms. The sites on the other sublattice are occupied by S atoms or are empty, the latter alternative being required to fulfill the first coordination sphere of a trigonal As or P site. The lattice parameter a is obtained by considering a P−S bond distance d_{PS} = 2.1 Å, in agreement with crystallographic data for these bonds, which in the zinc-blend structure corresponds to $a = 4d_{PS}/\sqrt{3}$.[19] For M_2 calculations, clusters of up to 60^3 zinc-blend cells were considered, and their P-available positions were randomly occupied according to the glass composition and density. Whenever appropriate, constraints arising from chemical or thermodynamic considerations can be imposed on the number of P−S−P contacts per structural unit during the random distribution of P atoms in the cluster.[14,15] For each randomly generated distribution of P, a value of M_2 is calculated. The procedure is repeated many times, to probe a significant number of configurations of P in the cluster. The resulting set of M_2 values is presented in the form of a histogram. The appropriate number of repetitions, dependent on the number of P atoms in the cluster, was determined by checking the stabilization of the shape of the histogram, typically between 30 000 and 50 000 repetitions.

II.2.c. Molecular-like P−S Clusters. If P atoms in the glass are forming well-defined molecular-like arrangements as observed in crystal phases, the ^{31}P homonuclear dipolar interaction should be an adequate tool to detect these units, due to the sensitivity of M_2 to the number of short P−P contacts. In previous studies using Raman spectroscopy, the possibility was suggested that in $As_2S_{3(1-x)}$−$P_2S_{5(x)}$ glasses there are well-defined molecular building blocks such as P_4S_{10} and $As_2P_2S_8$.[7] The ^{31}P second moment associated with a set of diluted molecules randomly oriented with respect to the magnetic field can be calculated using the Van Vleck expression 1. A complete modeling of the glass structure based on the occurrence of these species dispersed in an As−S network may give the possibility of checking the validity of this structural model by comparing the calculated M_2 with experimental values. In this work, we adopted a less demanding computational approach, which can still provide a useful hint for the magnitude of the dipolar coupling in these kinds of molecular arrangements. The minimum-energy structures of isolated $As_2P_2S_8$, P_4S_{10}, P_4S_9, and P_4S_7 units were calculated, running semiempirical PMM3 calculations with the quantum chemical package Spartan Pro 2.0.[20] With this optimized geometry, the dipolar coupling between the P atoms was calculated.

III. Experimental Procedures

III.1. Sample Preparation and Characterization. The glasses are prepared conventionally by heating the elements together in a sealed quartz tube at temperatures between 620 and 800 °C, depending on the glass composition. The starting materials used are As, P, and S having a purity of 99.999%, and thus glass composition having different amounts of P were prepared. First we prepared arsenic glass having the composition As_2S_3 as reported by Devyatykh,[2] and then phosphorus and sulfide were added according to the stoichiometry of the P_2S_5 compound. The amorphous character of the samples was confirmed by X-ray diffraction. The characteristic temperatures were determined by differential scanning calorimetry (DSC).

III.2. Preparation of Crystalline Phase $AsPS_4$. In order to have a crystalline system closely related to these glasses and also to

(18) Van Vleck, J. H. *Phys. Rev.* **1948**, *74* (9), 1168.

(19) Ashcroft, N.; Mermin, D. *Solid State Physics*; Brooks/Cole: New York, 1976.

(20) *Spartan pro 2.0*; Wavefunction Inc.: Irvine, CA, 2002.

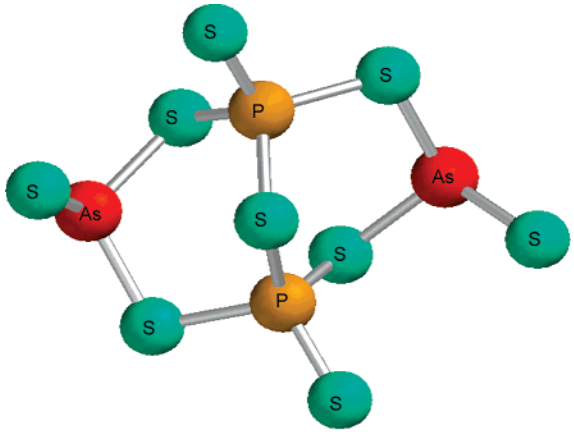

Figure 1. Molecular-like unit present in the structure of crystalline $AsPS_4$.[9]

Table 1. Physical Properties of Stoichiometric $As_2S_{3(1-x)}-P_2S_{5(x)}$ Glasses

			temperatures (°C)	
glass x (mol %)	D (g/cm^3)	V_m (cm^3/mol)	T_g	T_f
0	3.201	76.64	200	
0.1	2.998	81.27	194	
0.2	2.989	80.71	187	-
0.3	2.747	86.96	184	413
0.4	2.693	87.81	174	440
0.5	2.519	92.94	170	458
0.6	2.503	92.61	160	457
0.7	2.266	99.93	143	393

establish correlations between NMR parameters and a known crystal structure, a sample of the compound $AsPS_4$ was prepared. This compound corresponds to the stoichiometry of the glass with $x = 0.5$. According to the procedure described above, the components As, P, and S were mixed in stoichiometric proportions, heated to 800 °C for 48 h, cooled down to 250 °C, kept at this temperature for 4 h, and then cooled to room temperature. The presence of crystalline $AsPS_4$ was confirmed by comparing the powder X-ray diffraction pattern with reference data.[21] Considering the instability of the samples exposed to the atmosphere, the ampoules were opened, and the samples were powdered moments before carrying out the NMR measurements. Typically, ^{31}P NMR signals from decomposition of the samples packed into NMR rotors were detected only after some hours.

III.3. NMR Spectroscopy. High-resolution ^{31}P-MAS NMR spectra of some crystal and glass samples were measured in a magnetic field of 9.4 T with a spectrometer Varian Unity INOVA. Measurements were carried out under MAS of up to 13 kHz in silicon nitride rotors with $\pi/2$ pulses (4 μs length) and recycle delays of 800 s. Chemical shifts were referenced to a 85% H_3PO_4 solution. Static NMR experiments to determine the line shape and homonuclear dipolar second moment were (M_2) carried out in a field of 7.4 T using a Hahn spin−echo sequence with $\pi/2$ pulses (7 μs length), with pulse separations up to 2 ms and recycle delays of 800 s. The chemical shift tensor elements were evaluated using the Herzfeld-Berger method in MAS spectra and also from direct simulation of the static spectrum using a FORTRAN90 coded program.

IV. Results and Discussion

The glass compositions prepared in this study are summarized in Table 1, where their characteristic temperatures, glass transition temperature (T_g) melting temperature (T_f), density D, and molar volume (V_m) are also shown.

(21) International Centre For Diffraction Data. *Powder Diffraction file*: *release 2000*; Newtown Square, 2000. PDF n. 45-1233. CD-ROM.

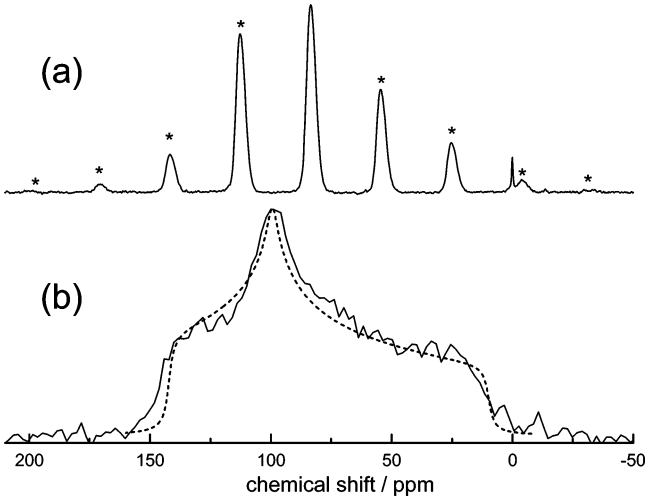

Figure 2. ^{31}P spectra of the crystalline $AsPS_4$ sample: (a) MAS and (b) static. Dotted line: simulation of the anisotropic spectrum. Asterisks: spinning side-bands.

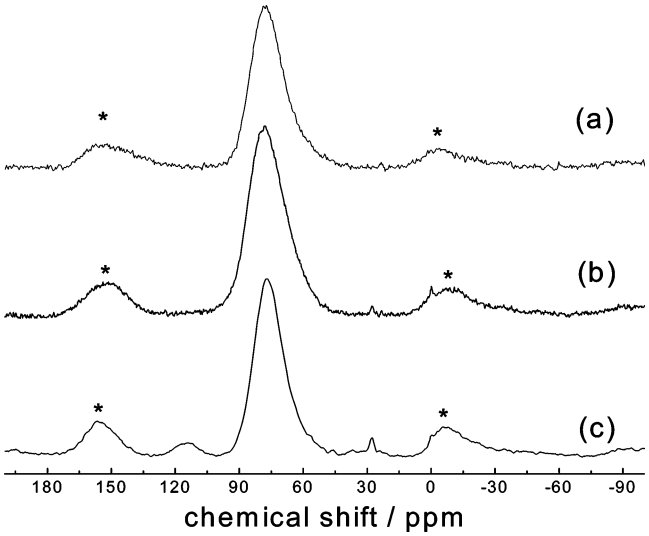

Figure 3. ^{31}P MAS NMR spectra of glasses: (a) $x = 0.1$, (b) $x = 0.4$, and (c) $x = 0.5$.

The values of T_g are comparable to previous studies by Tverjanovich (1991), where T_g decreases as the P content is increased.[7] Conversely, the melting temperature does not follow the same behavior as T_g, showing an increase up to $x = 0.5$ and then a gradual decrease above this concentration. Tverjanovich and co-workers attributed this behavior to the existence of two partial glassy systems, $As_4S_6-As_2P_2S_8$ and $As_2P_2S_8-P_4S_{10}$.[7] The molar volume increases as As atoms are replaced by P which is unexpected as the size of P^{3+} is smaller relative to As^{3+}. It might be proposed that this behavior reflects an increase in the average coordination number and a decrease in the degree of rigidity.

IV.1. ^{31}P NMR Spectroscopy. *IV.1.a. Crystallized $AsPS_4$.* Despite the full crystal structure of $AsPS_4$ not yet being resolved, it was determined that the building blocks are molecular-like $As_2P_2S_8$ groups, as shown schematically in Figure 1, having two $S{=}PS_{3/2}$ units.[9] These units are connected through As−S−As bridges, giving rise to a polymerized network.[9,7] The ^{31}P MAS and static spectra of

Table 2. ^{31}P Isotropic Chemical Shift and Chemical Shift Anisotropy Parameters for Glasses with $x = 0.1$ and $x = 0.5$ and for $AsPS_4$ Crystal

sample	method	$\delta_{iso}{}^a$ [ppm]	$\Delta\delta^b$ [ppm]	η^c	$\boldsymbol{\delta}_{11}$[ppm]	$\boldsymbol{\delta}_{22}$ [ppm]	$\boldsymbol{\delta}_{33}$ [ppm]
glass $x = 0.1$	static	80 ± 5	-90 ± 5	0.4 ± 0.1	150	113	−5
glass $x = 0.5$	static	87 ± 5	-95 ± 5	0.55 ± 0.05	170	115	−2
crystal $AsPS_4$	MAS	83.5 ± 0.2	-108 ± 5	0.6 ± 0.1	145	97	8
	static	83.0 ± 0.5	-111 ± 2	0.58 ± 0.03	141	99	9

$^a\delta_{iso} = {}^1/_3(\delta_{11}+\delta_{22}+\delta_{33})$. $^b\Delta\delta = \delta_{33} - {}^1/_2(\delta_{11}+\delta_{22})$. $^c\eta = (\delta_{22}-\delta_{11})/(\delta_{33}-\delta_{iso})$.

the crystallized sample are shown in parts a and b, respectively, of Figure 2. The MAS spectrum shows a single resonance at 83.5 ppm which agrees with previous NMR results.[22] The parameters for the chemical shift anisotropy interaction (CSA) were calculated from the Herzfeld-Berger analysis of the spinning sideband manifold in the MAS spectrum and also from the direct simulation of the static powder pattern, which is also shown in Figure 2b. The parameters obtained from both methods are shown in Table 2, where an excellent agreement is observed for the crystal.

It is interesting to compare the tensor elements in Table 2 with the known behavior for these quantities in $PS_{3/2}$ and $S{=}PS_{3/2}$ units. According to systematic NMR studies carried out in crystalline P_4S_x compounds, both species can be identified from the most shielded elements of the CSA tensor.[23] In $S{=}PS_{3/2}$ units, this element corresponds to the shielding along the P═S direction, with a value around −60 ppm. In contrast, for $PS_{3/2}$ units, all tensor elements have positive values, and the most shielded element takes values around 0 ppm.[23] Interestingly, in $AsPS_4$ which has only $S{=}PS_{3/2}$ units, the most shielded element has a value of about 9 ppm. This observation, which is in apparent disagreement with the expected correlation in P_4S_x series, is in fact demonstrating the strong effect of the As−S−P linkages and the structural distortions on the shielding of $S{=}PS_{3/2}$ units in the $As_2P_2S_8$ group. The high value of the asymmetry parameter, $\eta = 0.58$, indicates a considerable deviation from the axial symmetry around the direction of the P═S bond, which is consistent with the fact that in a low-symmetry molecular-like cage, the tetrahedral units should be considerably distorted with respect to the axial symmetry. On the other hand, the anisotropy parameter $\Delta\delta$ has a negative value, which is consistent with the values observed for tetrahedral $S{=}PS_{3/2}$ units.[24]

IV.1.b. Glasses in the As−P−S System. Figure 3 shows the ^{31}P-MAS spectra of some glass compositions. The most prominent feature of these spectra is the asymmetric line centered about 77 ppm. A substantially weaker line corresponding to 5% of the whole integral intensity is observed for the $x = 0.5$ glass at around 115 ppm. This line can be attributed to trigonal $PS_{3/2}$ units according to observations in the literature.[16,24] In some samples, weak and narrow lines are observed at around 27 ppm and 0 ppm, which corresponds to oxidation products arising from exposure to the atmosphere. Aside from a slight decrease in the asymmetry of the stronger peak, no significant variation of the isotropic spectrum was observed as the phosphorus content was increased. In order to discuss the origin of the stronger NMR line, the CSA parameters were determined for the $x = 0.1$ and $x = 0.5$ samples. For this reason, the static ^{31}P spectra of these glasses were measured with the spin−echo sequence $\pi/2$-150 μs-π, as shown in Figure 4. The CSA tensor elements were obtained from the simulation of these spectra and are summarized in Table 2. Despite the static spectra being considerably broadened, mainly by the homonuclear P−P interaction and the distribution of interaction parameters caused by disorder, the agreement of the simulation is good. The effect of the distribution of coupling parameters is considered in the simulation through the broadening of the function convoluted with the spectral density. This convolution function was assumed as a Gaussian with a broadening adjusted to 1.8 kHz. Similar CSA parameters were also estimated from the Herzfeld-Berger analysis of the MAS spectra. However, the uncertainty of these results is higher because the considerable line broadening in the glasses prevented the reduction of the spinning speed to the lower values required for optimum application of the method. For this reason, only the CSA parameters extracted from the static spectra were considered.

As can be seen in Table 2 there are no significant differences between the glasses for the values of the CSA anisotropy ($\Delta\delta$) and the isotropic shift (δ_{iso}). On the other hand, the asymmetry parameter (η) increased from 0.4 for glass $x = 0.1-0.6$ for glass $x = 0.5$. The set of CSA parameters for the $x = 0.5$ glass is quite similar to that measured for the crystallized sample with $x = 0.5$, indicating that the phosphorus structural units present in the glass are very nearly the same as those in the crystallized sample. For this reason, it is possible to conclude that the main phosphorus groups in the glass are $S{=}PS_{3/2}$ within a cyclic $As_2P_2S_8$ unit. The smaller value of η in the glass whose $x = 0.1$, corresponding to an $S{=}PS_{3/2}$ tetrahedra in a slightly more symmetric conformation, indicates a certain degree of sensitivity of the $As_2P_2S_8$ units to the structural environment at the medium-range scale. In glasses with a low concentra-

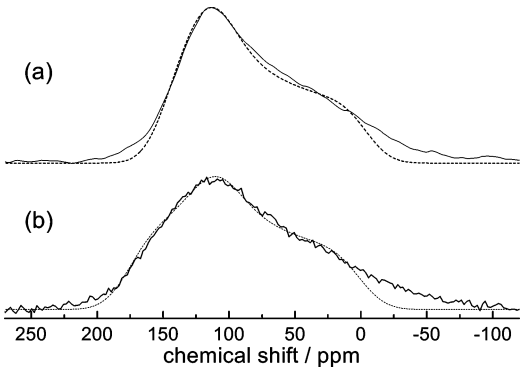

Figure 4. Static ^{31}P-NMR spectra for glasses: (a) $x = 0.1$ and (b) $x = 0.5$. Dashed lines: simulation of the CSA powder pattern.

(22) Aitken, B. G.; Youngman, R. E.; Ponader, C. W. *J. Non-Cryst. Solids* **2001**, *284*, 34.
(23) Eckert, H.; Liang, C. S.; Stucky, G. D. *J. Phys. Chem.* **1989**, *93*, 452.
(24) Cherry, B. R.; Zwanziger, J. W.; Aitken, B. G. *J. Non-Cryst. Solids* **2004**, *333*, 28.

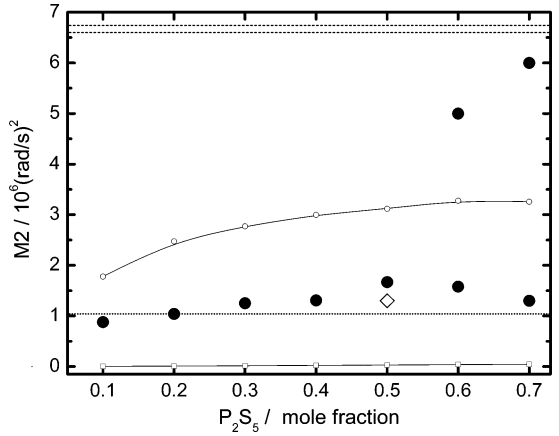

Figure 5. ^{31}P-Homonuclear second moment M_2 as a function of composition and calculation for model distributions of P. Filled circles: experimental data for glasses. Diamond: Experimental value for crystallized sample ($AsPS_4$). Blank squares: homogeneous dispersion of P. Blank circles: Random distribution of P. Straight lines: M_2 calculated for isolated molecular-like units, with structure modeled by semiempirical PM3 method. Dotted line: $As_2P_2S_8$ group. Dashed lines: P_4S_9 and P_4S_{10}.

tion of P, this environment corresponds to units dispersed in a network of trigonal groups $AsS_{3/2}$, while for higher concentration of P $As_2P_2S_8$ groups may be closer or even linked by As−S−As bridges.

IV.2. ^{31}P-Homonuclear Dipolar Interaction. Figure 5 shows the resulting values for M_2 as a function of the glass composition, obtained from least-square fittings to the observed spin−echo decays. For the sake of comparison, the M_2 value for the crystallized sample with $x = 0.5$ is also shown in Figure 5. For glasses up to $x = 0.5$, the whole echo decay was well reproduced by a single Gaussian function, as in expression 2. However, for glasses with x above 0.5, the decays were clearly non-Gaussian. In these cases, the fitting of a sum of two Gaussian functions gave excellent results, indicating the existence of two local spin groupings with substantially different values of M_2, as can be seen in Figure 5 for $x = 0.6$ and $x = 0.7$.

Figure 5 also shows the results from the calculation of M_2 according to the proposed P distributions. The calculation done for a homogeneous distribution of P in the glass matrix gave M_2 values of at least 1 order of magnitude less than the experimental ones, starting from 0.002×10^6 rad^2 s^{-2} for $x = 0.1$, to 0.044×10^6 rad^2 s^{-2} for $x = 0.7$. For this reason, a homogeneous dispersion of P atoms in an As−S network can be easily disregarded for these glasses.

On the other hand, the calculations using the random distribution model were carried out, imposing the constraint of one P−S−P bridge at the most around each P atom in the zinc-blend framework. This was done in this way because the results obtained from simulations without constraints gave values of M_2 substantially higher than the experimental ones, indicating that these configurations with several P−S−P bonds per unit are not formed in the glasses. Figure 6 shows the normalized histograms for M_2 as a function of the glass composition. Two peaks can be observed in these distributions. The peak corresponding to M_2 values less than 10^6 rad^2 s^{-2} is associated with clusters having no P−S−P contacts. The peak for M_2 values above 2.5×10^6 rad^2 s^{-2} corresponds to configurations having P sites with a single

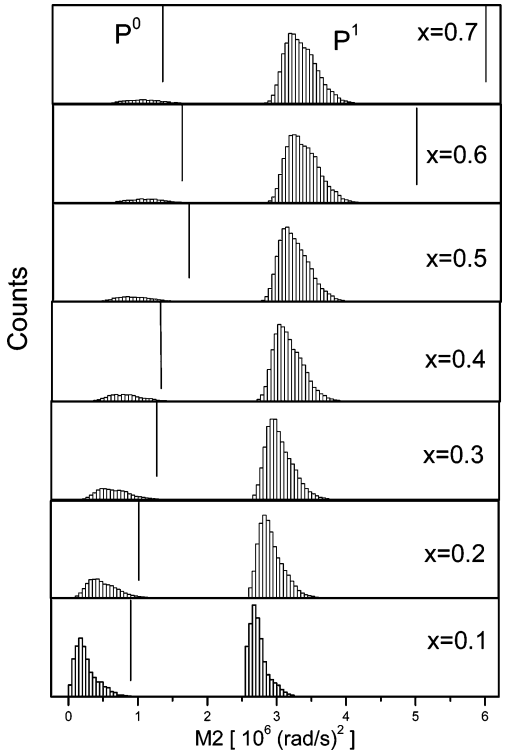

Figure 6. Histograms of M_2 values resulting from calculations of randomly distributed P, as a function of the glass composition. Vertical lines: experimental values. P^0 and P^1: phosphorus environments with 0 or 1 P-S-P bridge, respectively.

P−S−P contact per unit. We will identify these two kinds of P environments respectively as P^0 and P^1, where the superscript indicates the number of P−S−P bridges for that specific P-site. The vertical lines in Figure 6 indicate the experimental M_2 values for the corresponding composition. The mean M_2 values calculated from these histograms are plotted in Figure 5 as a function of the composition.

According to data in Figure 6, except for the glass with $x = 0.1$, the most probable phosphorus neighborhood includes one P−S−P contact, and for this reason the mean M_2 is mostly governed by the values corresponding to P^1. These M_2 values have the same order of magnitude as the experimental results but are higher by a factor of 3. Considering the limitations of the model, the degree of approximation to the observed M_2 can be considered satisfactory. The disagreement can be attributed mainly to the lack of an accurate estimation of the r_{PP} interatomic distances as well as the effect of next nearest neighbors. According to the r_{PP}^{-6} dependence in the Van-Vleck expression, a variation of 20% in r_{PP}^{-6} causes a variation by a factor of 3 in M_2, without considering the contributions of more distant neighbors. In order to pursue a closer comparison with the experiment, a more refined structural model of the glass should be worked out. The conclusion that can be drawn from these calculations is that, at the level of P incorporation in these glasses, P^0 environments are less likely to be found than P^1. Conversely, species P^n with $n > 1$, though statistically probable, are certainly not found in glasses with $x \leq 0.5$.

According to the conclusions obtained from the analysis of the ^{31}P NMR spectra in section IV.1.b, the presence of $As_2P_2S_8$ units should be contrasted with the measured values

of M_2. These molecular groups are compatible with the previous M_2 calculations, indicating that the P^1 species are more likely to be found. The minimum energy conformations for $As_2P_2S_8$ isolated groups were calculated, giving P−P interatomic distance values of $r_{PP} = 3.79$ Å and a P−S−P angle of $\beta = 124.27°$. The resulting P−S bond lengths (2.162 Å and 2.095 Å) and P═S (1.88 Å) are compatible with values observed in many compounds containing P and S. From these structural parameters, the resulting value for M_2 is 1.04×10^6 rad^2 s^{-2}. For the sake of comparison, this quantity was represented in Figure 5 as a horizontal dot line, showing good agreement with the experimental data, especially for glasses with lower P concentration. This calculation has two obvious limitations: the contributions to the M_2 from P atoms in neighboring molecules are not included, and the molecular conformation corresponds to a completely relaxed unit. To evaluate the influence of these factors in the calculated M_2 of the $As_2P_2S_8$ unit, it is interesting to compare the values of M_2 measured in the $x = 0.5$ glass (1.67×10^6 rad^2 s^{-2}) and the corresponding crystal (1.30×10^6 rad^2 s^{-2}). It is expected that in the crystal, with a more compact molecular packing compared to the glass, P−P distances between intermolecular units will be shorter, leading to stronger dipolar couplings. However, the M_2 values show the opposite behavior, indicating that the observed variation in M_2 cannot be attributed to an increase in dipolar coupling from neighboring molecules but to distortions in the conformation of the $As_2P_2S_8$ unit.

Let us now consider the minimum energy conformation of the isolated unit having the lowest M_2 and consequently the largest distance r_{PP}. More strained conformations, due to the effect of the molecular packing, causing a reduction in r_{PP} would lead to higher M_2 values, as observed in the crystal (30% higher) and the glass (60% higher). Therefore, variations of approximately 0.3×10^6 rad^2 s^{-2} can be readily attributed to strained molecular conformations. This amount of variation is compatible with the observed increase in M_2 as a function of the P content in the glass. For these reasons, it should be concluded that the observed increase in M_2 of up to $x = 0.5$ may be caused by a combination of an increasingly distortion in the $As_2P_2S_8$ units, reducing the P−S−P angle, and the dipolar coupling with P in neighboring units.

Table 3. Values of M_2 Calculated for Some Isolated Molecular Units, Corresponding to Conformations Optimized from Semiempirical Methods

unit	M_2 (rad^2 s^{-2})
$As_2P_2S_8$	1.04×10^6
P_4S_{10}	6.63×10^6
P_4S_9	6.74×10^6
P_4S_7	30.4×10^6

Table 3 shows the M_2 values for P_4S_{10}, P_4S_9, and P_4S_7 units, resulting from the calculated minimum energy conformation. The values are substantially higher than the experimental ones for glasses whose $x \leq 0.5$ but are comparable with the highest M_2 measured for glasses with $x = 0.6$ and 0.7. This observation indicates that local P−S arrangements with more than one P−S−P bridge are formed in these glasses. On the other hand, the presence of molecular units having direct P−P bonds, such as P_4S_7, can be excluded in this range of concentrations due to the substantially higher value of M_2 associated with them which is not compatible with the experimental results.

V. Conclusion

According to the ^{31}P NMR experiments and calculations, the phosphorus atoms in $As_2S_{3(1-x)}$−$P_2S_{5(x)}$ glasses are incorporated in the structure through the formation of molecular-like units dispersed in an As_2S_3 matrix. For compositions with low values of P_2S_5, dispersed $As_2P_2S_8$ units are formed, which become progressively interconnected as the P concentration approaches $x = 0.5$, where they establish a fully polymerized structure. The possibility of some $S{=}PS_{3/2}$ groups forming P−S−P contacts outside well-defined $As_2P_2S_8$ cages may not be disregarded from the NMR point of view as long as the P−P distance is similar than in the cages. For glasses with $x > 0.5$, there is a coexistence of $As_2P_2S_8$ groups with molecular units connecting more P atoms via P−S−P bridges, such as P_4S_{10} or P_4S_9 units. No evidence of structures composed by P−P bonds was found. This behavior also clearly explains the decrease of T_g and the increase of molar volume as P_2S_5 increases, which indicates that the dominant species is $S{=}PS_{3/2}$, which is present in the $As_2P_2S_8$ molecular unit.

Acknowledgment. The authors would like to thank CNPq and FAPESP for financial support.

CM070496K